Quantitative attribution of climate effects on Hurricane Harvey's extreme rainfall in Texas

Environmental Research Letters

LETTER

Quantitative attribution of climate effects on Hurricane Harvey's extreme rainfall in Texas

S-Y Simon Wang[1,2], Lin Zhao[3], Jin-Ho Yoon[4,6], Phil Klotzbach[5] and Robert R Gillies[1,2]

[1] Utah Climate Center, Utah State University, Logan, UT, United States of America
[2] Department of Plants, Soils, and Climate, Utah State University, Logan, UT, United States of America
[3] Key Laboratory of Land Surface Process and Climate Change in Cold and Arid Regions, Northwest Institute of Eco-Environment and Resources, Chines Academy of Sciences, Lanzhou, People's Republic of China
[4] School of Earth Sciences and Environmental Engineering, Gwangju Institute of Science and Technology, Gwangju, Korea
[5] Department of Atmospheric Science, Colorado State University, Ft. Collins, CO, United States of America
[6] Author to whom any correspondence should be addressed.

E-mail: yjinho@gist.ac.kr

OPEN ACCESS

RECEIVED
4 December 2017

REVISED
16 March 2018

ACCEPTED FOR PUBLICATION
4 April 2018

PUBLISHED
30 April 2018

Keywords: Hurricane Harvey, global warming, downscaling attribution, extreme event

Supplementary material for this article is available online

Abstract

Hurricane Harvey made landfall in August 2017 as the first land-falling category 4 hurricane to hit the state of Texas since Hurricane Carla in September 1961. While its intensity at landfall was notable, most of the vast devastation in the Houston metropolitan area was due to Harvey stalling near the southeast Texas coast over the next several days. Harvey's long-duration rainfall event was reminiscent of extreme flooding that occurred in the neighboring state of Louisiana: both of which were caused by a stalled tropical low-pressure system producing four days of intense precipitation. A quantitative attribution analysis of Harvey's rainfall was conducted using a mesoscale atmospheric model forced by constrained boundary and initial conditions that had their long-term climate trends removed. The removal of the various trends of the boundary and initial conditions minimizes the effects of warming in the air and the ocean surface on Harvey. The 60 member ensemble simulations suggest that post-1980 climate warming could have contributed to the extreme precipitation that fell on southeast Texas during 26–29 August 2017 by approximately 20%, with an interquartile range of 13%–37%. While the attribution outcome could be model dependent, this downscaling approach affords the closest means possible of a case-to-case comparison for event attribution, complementing other statistics-based attribution studies on Harvey. Further analysis of a global climate model tracking Harvey-like stalling systems indicates an increase in storm frequency and intensity over southeast Texas through the mid-21st century.

1. Introduction

Hurricane Harvey made landfall in Texas as a category 4 hurricane on the Saffir–Simpson wind scale and caused at least 73 direct fatalities with an estimated 30 000 people displaced from their homes. The catastrophic flooding produced by Harvey destroyed 9000 homes and damaged 185 000 additional homes (Texas Department of Public Safety). Total economic damage from Hurricane Harvey is estimated at between $90–$160 billion dollars (Blake and Zelinsky 2018). Scientific discussions soon emerged citing that the increased sea surface temperature (SST) in the Gulf of Mexico, the ability of the warmer troposphere to hold more moisture, and the growing stagnation of the atmospheric circulation feasibly, in unison, could strengthen the intensity of Harvey while worsening its impact (e.g. The Guardian, 8/28/2017; Potsdam Institute for Climate Impact Research, 8/28/2017). Subsequent attribution studies indicated an increase in extreme rainfall probability in Texas ranging from 15% (van Oldenborgh *et al* 2017) to 30% (Risser and Wehner 2017) that was linked to anthropogenic warming in the atmosphere, with an associated shortening of return periods for such precipitation events (Emanuel 2017).

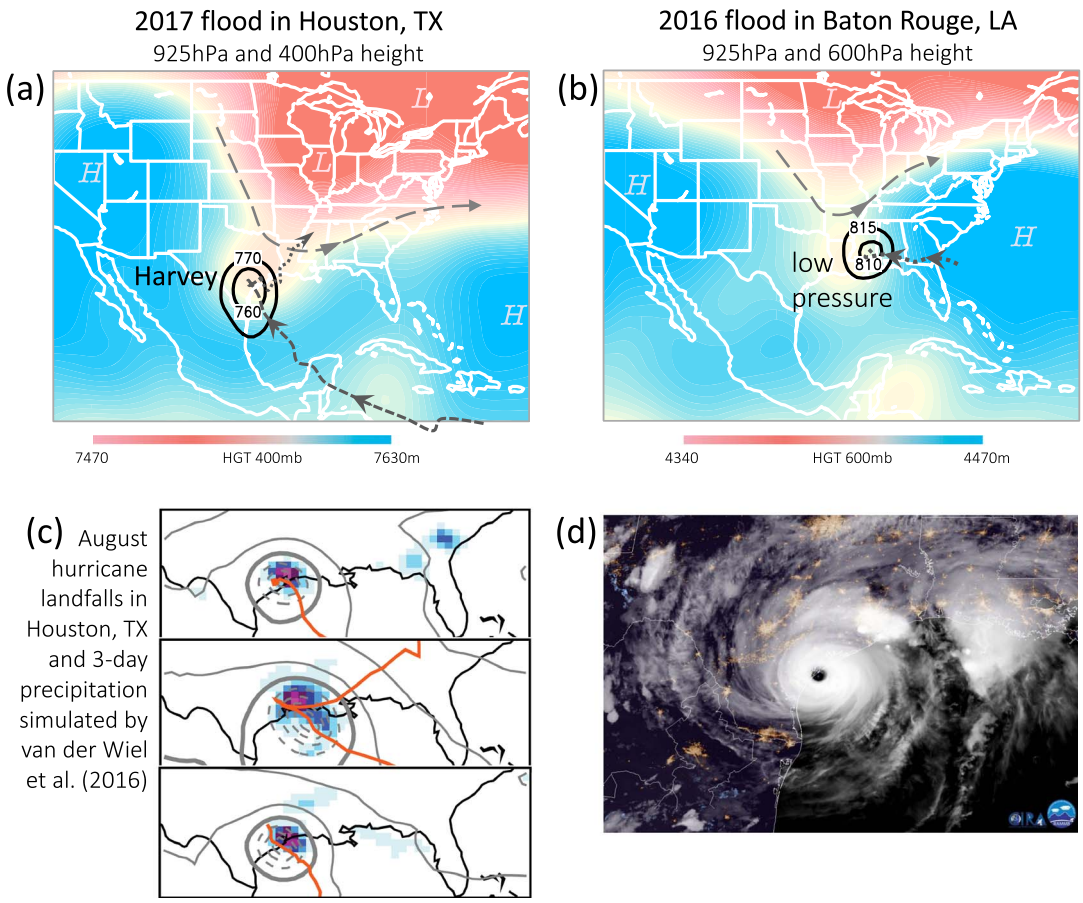
2017 flood in Houston, TX
925hPa and 400hPa height
(a)
H
L
L
H
770
Harvey
760
7470
HGT 400mb
7630m
2016 flood in Baton Rouge, LA
925hPa and 600hPa height
(b)
L
H
815
low
810
pressure
H
4340
HGT 600mb
4470m
(c) August hurricane landfalls in Houston, TX and 3-day precipitation simulated by van der Wiel et al. (2016)
(d)

Figure 1. (*a*

2. Harvey's meteorological history

Hurricane Harvey was first classified as a tropical depression on 17 August at 6 Z and was upgraded to a tropical storm that same day at 18 Z (Blake and Zelinsky 2018). Strong northeasterly shear, dry air entrainment and rapid storm translation speed contributed to weakening, and Harvey degenerated into an open tropical wave on 19 August while tracking through the eastern Caribbean. After moving across the remainder of the Caribbean and the Yucatan Peninsula as an open wave, Harvey encountered a much more conducive dynamic and thermodynamic environment when it entered the Bay of Campeche. It was upgraded to a tropical depression on 23 August at 12 Z and a tropical storm six hours later. Harvey tracked northward across the Gulf of Mexico and rapidly intensified in an environment of very low vertical wind shear and ~30 °C sea surface temperatures. During the 48 hour period from 24 August at 0 Z to 26 August at 0 Z, Harvey rapidly intensified by 75 knots. It made landfall shortly thereafter between Port Aransas and Port O'Connor, Texas as a 115 knot category 4 hurricane, with a central pressure at landfall of 937 hPa (figure 1(*d*)). The extreme precipitation that fell on southeast Texas was due to Harvey's stalling characteristics over the next several days—caused by collapsing steering currents. Anomalous high-pressure areas to the northwest and northeast of Harvey resulted in very weak steering over the storm itself (*ref.* steering current—figure 1(*a*)), and Harvey drifted very slowly eastward and then southeastward until it became caught up by a dipping upper-level trough, reversing its track. By 28 August, Harvey had drifted back out over the Gulf of Mexico and continued tracking slowly east-northeastward over the extreme western portion of the Gulf of Mexico over the next two days. By early 30 August, Harvey made its final landfall in Cameron Parish, LA as a weak tropical storm and weakened as it moved further inland (Blake and Zelinsky 2018).

Harvey's landfall ended the longest-running United States major (category 3+) hurricane landfall drought on record that had been ongoing since Hurricane Wilma in 2005 (Hart *et al* 2016). It was the first land-falling category 4 hurricane to hit the state of Texas since Hurricane Carla in 1961. Harvey's landfall pressure of 937 hPa was also the lowest for any hurricane in the Gulf of Mexico hurricane since Rita in 2005. Large parts of the Houston metropolitan area received over 30 inches of rain from Harvey, with a United States record of 60.58 inches recorded in Nederland, Texas. Harvey's proximity to the Gulf of Mexico allowed it to tap into copious amounts of moisture that inundated the Houston metropolitan area triggering catastrophic flooding.

3. Data and modeling approach

3.1. Data sources

Harvey's meteorological history was summarized from the National Hurricane Center best track report (Blake and Zelinsky 2018). Observed precipitation data were derived from the 4 km NCEP Stage-IV Quantitative Precipitation Estimates (Lin and Mitchell 2005). For sea surface temperatures, we used the Extended Reconstructed Sea Surface Temperature (ERSST) version 4. The NCEP-NCAR Reanalysis-1 data (R1) and the NCEP-DOE Reanalysis 2, or R2 (Kanamitsu *et al* 2002) were used to depict the atmospheric variables and to compute the trends. For future climate projections, we analyzed the Community Earth System Model version 1 (CESM1) under the Large Ensemble (LE) Project (Kay *et al* 2015). We used the LE simulations for the 2006–2080 period with RCP8.5 forcing, producing 40 members with selected daily variables at a spatial resolution of 0.9° long. × 1.25° lat.

3.2. Regional model

Simulations using the Advanced Research Weather Research and Forecasting (WRF-ARW) model (Skamarock and Klemp 2008) version 3.8 were performed for the heavy precipitation period over southeast Texas from 0000 UTC 26 August to 0000 UTC 30 August 2017. The model was forced by initial conditions (IC) and lateral boundary conditions (LBC) using the 0.5° × 0.5°-resolution Global Forecast System (GFS) initial analysis. We focused on the post-1980 trend in both tropospheric and ocean surface temperature and conducted four experiments: (1) A control simulation forced by the original GFS analysis as IC and LBC, and a set of 'detrended' simulations in which we removed the linear trends from the IC and LBC for (2) SST (denoted as DSST), (3) all tropospheric variables (DAIR), and (4) both SST and tropospheric variables (DSST+DAIR). The trends were first computed from the R2 monthly data for each variable and then linearly interpolated onto the GFS's resolution and pressure levels. Then, we subtracted these trends from the GFS's initial analysis (geopotential height, horizontal winds, air temperature, etc.) before using it as IC and LBC to drive the WRF-ARW. To evaluate model sensitivity, we also added a double-trend simulation forced by the original LBC to which the post-1980 trends in both the atmosphere and SST were added instead of removed, hence 'doubling' the warming effect; this is denoted as DB runs.

The assumption here is that any post-1980 trend manifest in the troposphere and ocean surface contains signals that are traceable to anthropogenic global warming, which is supported by most attribution analysis (Weaver *et al* 2017). Of course, we also had to assume that Harvey would occur anyway within the climatically detrended environment. This 'detrended

Table 1. Twenty combinations of different cumulus schemes and microphysics in WRF-ARW v3.8 (omitting references due to page limits), which were run at three spatial resolutions of 10, 15 and 20 km.

No	Cumulus schemes	Microphysics
1	Kain–Fritsch	Kessler
2	Betts–Miller–Janjic	Kessler
3	Modifed Tiedtke	Kessler
4	New GFS simplified Arakawa-Schubert	Kessler
5	Kain–Fritsch	Lin
6	Betts–Miller–Janjic	Lin
7	Modifed Tiedtke	Lin
8	New GFS simplified Arakawa-Schubert	Lin
9	Kain–Fritsch	WSM-3
10	Betts–Miller–Janjic	WSM-3
11	Modifed Tiedtke	WSM-3
12	New GFS simplified Arakawa-Schubert	WSM-3
13	Kain–Fritsch	Ferrier (new Eta)
14	Betts–Miller–Janjic	Ferrier (new Eta)
15	Modifed Tiedtke	Ferrier (new Eta)
16	New GFS simplified Arakawa-Schubert	Ferrier (new Eta)
17	Kain–Fritsch	Thompson
18	Betts–Miller–Janjic	Thompson
19	Modifed Tiedtke	Thompson
20	New GFS simplified Arakawa-Schubert	Thompson

downscaling' approach follows that used by Cho *et al* (2016) for the attribution analysis of the June 2013 flood in northern India and the role climate warming played in that event. To assess simulation uncertainty, the WRF-ARW model was run with 60 members in each of the four experiments; these encompass 20 combinations from four microphysics schemes and five cumulus parameterization schemes (listed in table 1) that were run at three spatial resolutions: 15, 20, and 25 km ($4 \times 5 \times 3 = 60$ members). We used a single domain centered around Houston, TX (30°N, 95°W) with the domain outlined in figure 3. To better depict the environmental conditions and associated changes from the detrending, we enabled the '3 dimensional analysis and surface nudging' of WRF-ARW in all of the experiments.

4. Results

4.1. WRF-ARM attribution

In the Gulf of Mexico (defined as 100-80°W, 20–30°N), August SST has warmed by ~0.7 °C since 1980 (figure 2(*a*) red line), while the lower tropospheric temperature within the 1000−500 hPa layer has warmed by 1.4 °C through 2017 (figure 2(*b*), based on R1 data). Precipitable water over the Gulf of Mexico has increased by 7.3% since 1980 with August 2017 being the highest monthly value per R1 data (figure 2(*c*)). In the WRF-ARW detrended experiments (2)−(4), such post-1980 trends were removed from all the meteorological variables in the IC and LBC. We refer to these simply as climate trends rather than global warming trends, since it is likely that not all of the SST increase in the Gulf of Mexico since 1980 is due to anthropogenic causes. The Atlantic Multi-decadal Oscillation, for example, has a pronounced signal in the Gulf of Mexico (Enfield *et al* 2001), as is evidenced in the multi-decadal variability of SST (figure 2(*a*)) embedded in the long-term warming trend. On the other hand, the warming after 1990 did start to exceed the spread of variability as shown by the CESM1 historical experiment ensembles in both the SST (figure 2(*d*)) and lower-tropospheric temperature (figure 2(*e*)), suggesting a prominent role of anthropogenic warming.

Harvey produced extremely heavy rainfall in southeast Texas during 26−29 August 2017. The four-day average of 700 h Pa geopotential height and accumulated precipitation from 26−29 August, produced by the control simulation from the ensemble of 60 members, are shown in figure 3(*b*) and are compared with the observed precipitation and the 12 km North American Mesoscale model initial data in figure 3(*a*). The simulated center of Harvey is very close to its actual location but the precipitation centers are shifted about 120 km to the southwest of the observed—a persistent bias. The patterns of accumulated precipitation in DSST, DAIR, DSST+DAIR and DB (figures 3(*c*)−(*f*)) follow the slightly shifted precipitation of the control run and are more concentrated near the hurricane center than the observation (figure 3(*a*)). Nevertheless, the metropolitan area of Houston is within the simulated precipitation maxima indicating that model bias is minimal in our assessment.

The box and whisker diagram in figure 4(*a*) shows the median and spread of the 26−29 August accumulated precipitation *ratio* compared to the observation, averaged over southeast Texas (red box in figure 3). Based on the median, the control precipitation ensemble is only 1% smaller than the observation with an interquartile range from −12% to +8% and we considered this a reasonable simulation. Compared to the control run, the change in the simulated precipitation in southeast Texas was a 3% reduction in DSST, a 17% reduction in DAIR, and a 20% reduction in DSST+DAIR with an interquartile range of 10%−35%. In the double-trend experiment (DB), the precipitation median was increased by 9% with the upper quartile exceeding 20%. Since Harvey lingered along the Gulf Coast through 30 August, we also tested the daily precipitation accumulated through 27−30 August (see supplemental figure S1 available at stacks.iop.org/ERL/13/054014/mmedia). For this later period, the median change was a 9% reduction in DSST, a 22% reduction in DAIR, and a 26% reduction in DSST+DAIR while the DB experiment increased the precipitation by 10%—these are more robust change than from 26−29 August. It is noteworthy in the DSST+DAIR experiment of 27−30 August (figure S1) that even the upper extreme was lower than the observation, implying that climate warming can induce even more precipitation from hurricanes as strong as Harvey.

The impact of the climate trends on Harvey's strength was examined in terms of the central pressure difference from the observation during the 4 day

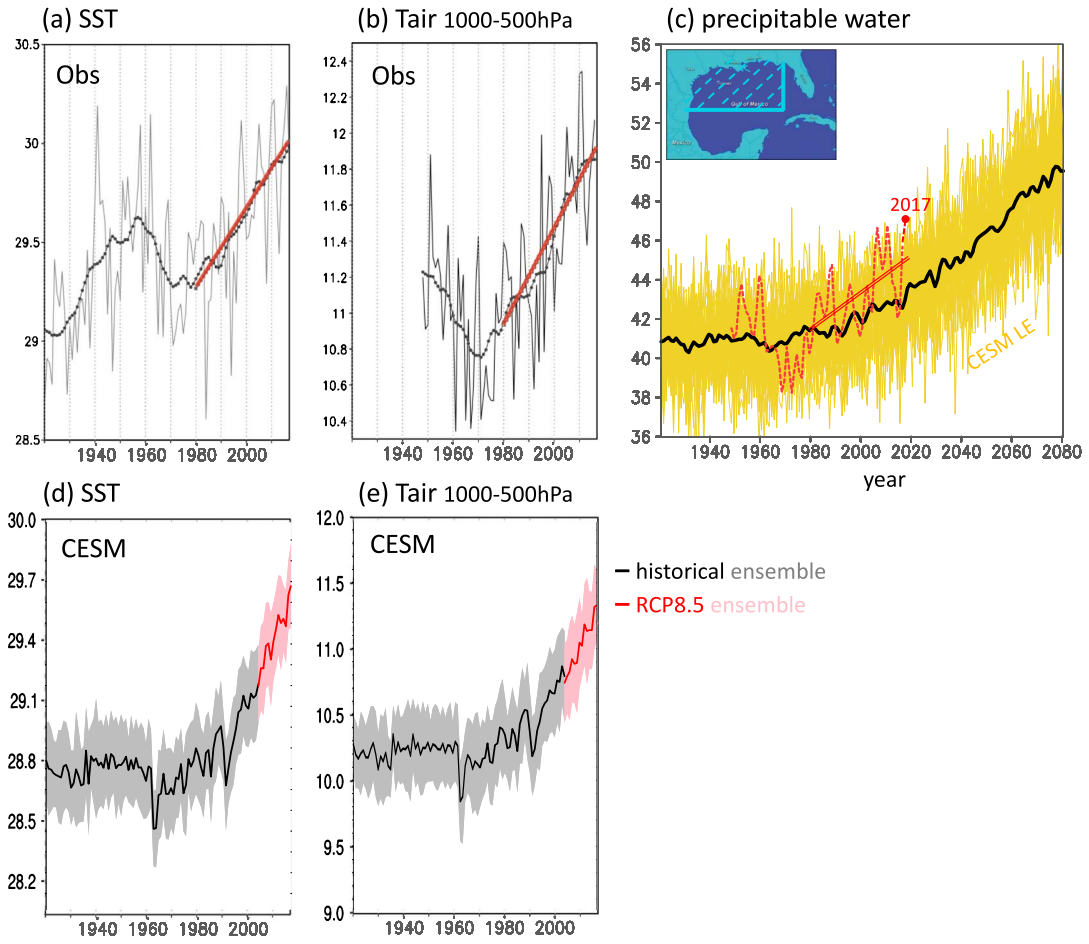

Figure 2. Observed August (*a*) SST and (*b*) air temperature in °C averaged from 1000−500 hPa overlaid with linear trends, as well as CESM LE (yellow) and observed (red) precipitable water over the Gulf of Mexico as outlined by the inset map. Black line in (*c*) is the 30 year running mean. (*d*) and (*e*) Same as (*a*) and (*b*) but from the CESM1 LE data.

period, which is shown in figure 4(*b*). Based on the median, the control run underestimated the center pressure by 2 hPa and DSST increased the pressure slightly from the control run by 0.3 hPa. The differences between control and both DAIR and DSST+DAIR are much more pronounced, increasing the center pressure by 5−6 hPa during 26−29 August (8 hPa during 27−30 August; figure S1). In DB, the center pressure was 2.5 hPa lower than the observed while the lower quartile was 6 hPa lower, suggesting that additional SST warming could intensify future Harvey-like hurricanes even further. The daily breakdown of these precipitation and central pressure comparisons is displayed in supplemental figure S2; the reduction effects of DAIR and DSST+DAIR had on Harvey's precipitation and central pressure are consistent. These results uniformly indicate the strengthening effect of the climate trends on Harvey.

Notable is the impact of DAIR on Harvey's precipitation and intensity which is much stronger than that of DSST, implying that climate trends in the atmospheric BC are critical in influencing Harvey. To infer the possible physical processes involved, we examined the post-1980 trends in the 300 hPa and 900 h Pa geopotential height, shown in supplemental figures S3(*a*) and S3(*b*). The increased upper-level height accompanying the decreased low-level height suggests an increase in the atmospheric thickness, likely associated with the mid-level warming; this is shown to be the case by a significant positive air temperature trend at 500 hPa (figure S3(*c*)). Such an increase in the atmospheric thickness and mid-tropospheric warming coincides with the vertical structure of a developing tropical cyclone which can be found on www.usno.navy.mil/NOOC/nmfcph/RSS/jtwc/pubref/References/GUIDE/chap4img/fig402.jpg and arguably contributes to the intensification of hurricanes.

4.2. Projection of the stalled storm

What is displayed in figure 1(*a*) describes an encounter between two sub-synoptic weather systems moving in opposite directions over Texas. Such weather systems are not uncommon but are random in nature. A case such as this fits the description of a classic tropical-extratropical interaction that combines abundant moisture carried with the low-pressure system and a vorticity source associated with the upper trough. Like the 2016 stalled cyclone that inundated portions of Louisiana (figure 1(*b*)), the upper trough moving through the central US induced a positive vorticity

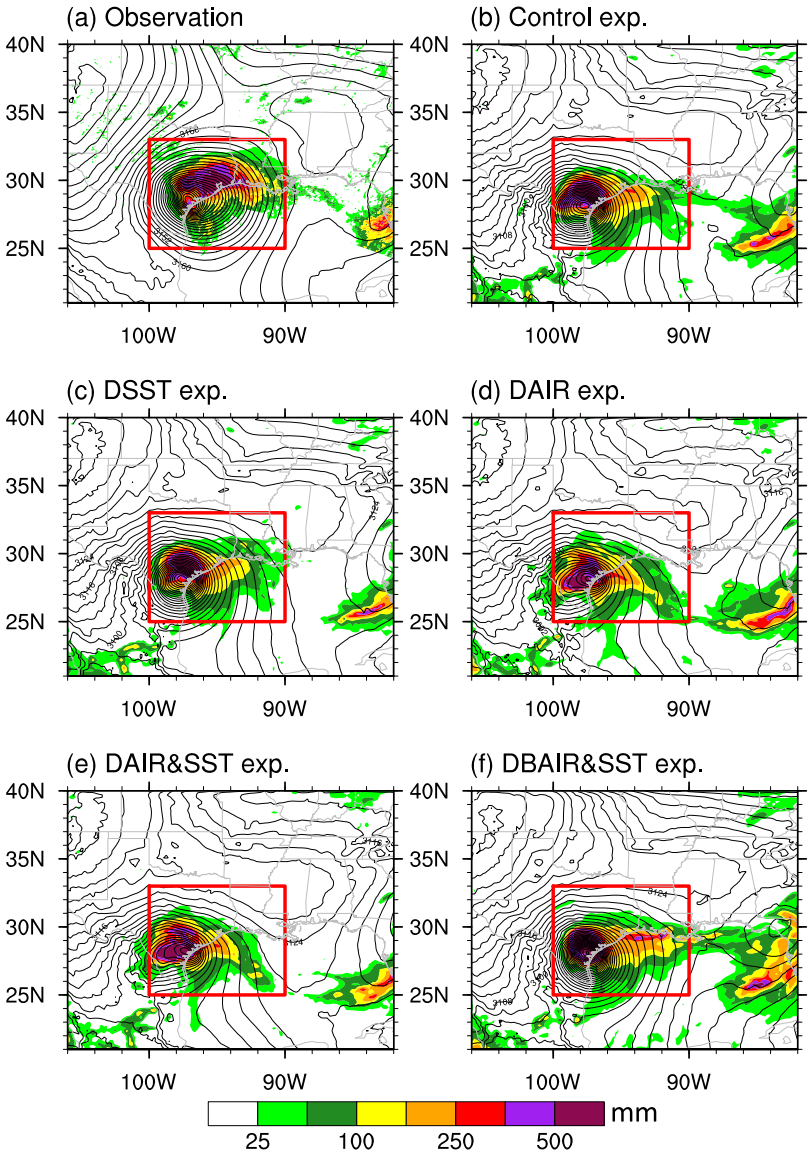

Figure 3. 26–29 August average of 700 hPa geopotential height (contour) and precipitation (shading) from (*a*) the observations of NAM initial and Stage IV and from the ensembles of (*b*) control, (*c*) DSST, (*d*) DAIR, (*e*) DAIR+DSST, and (*f*) double-trend/DB experiments. The red box is used for the domain average shown in figure 4.

tendency that intercepted the low-pressure system, inducing vortex stretching in the lower levels (Wang *et al* 2016). To provide a synoptic perspective, we tracked similar weather systems that resembled the unusual encounter of Harvey and the approaching cyclone that stalled it. A similar analysis was done by Wang *et al* (2016) for the August 2016 Louisiana stalled cyclone, and the ensuing analysis follows their method.

To identify similar cases involving a stalled storm along the Gulf Coast interacting with a dipping synoptic trough from the north, we conducted the analysis based upon the 26–29 August average conditions. We applied a spatial harmonic analysis to the four day geopotential height at 850 hPa to filter out zonal wavenumbers 8 and beyond, based upon the size of landfalling Harvey (~15° longitude in diameter); this spatial filter isolated the stalled Harvey as a low-pressure anomaly while eliminating ambient large-scale circulations such as the Bermuda High. We then applied a low-pass filtering for the 300 h Pa geopotential height by retaining wavenumbers 1–8; this was to depict the synoptic-scale flow pattern consisting of the western ridge and the eastern trough flow pattern, like the synoptic setting shown in figure 1(*a*), while removing shorter waves. This spatial filtering analysis was applied to both the R2 and CESM1 data.

Next, to objectively assess the extent to which any historical and simulated storm compares with Harvey, we adopted the 'pattern correlation coefficient' that calculates the Pearson product-moment coefficient of linear correlation between two variables at corresponding locations; this method outputs a single number (correlation coefficient denoted as ρ_P) that conveniently depicts the similarity between two systems. We computed ρ_P of the R2 geopotential height during 26–29 August with any four day mean of the

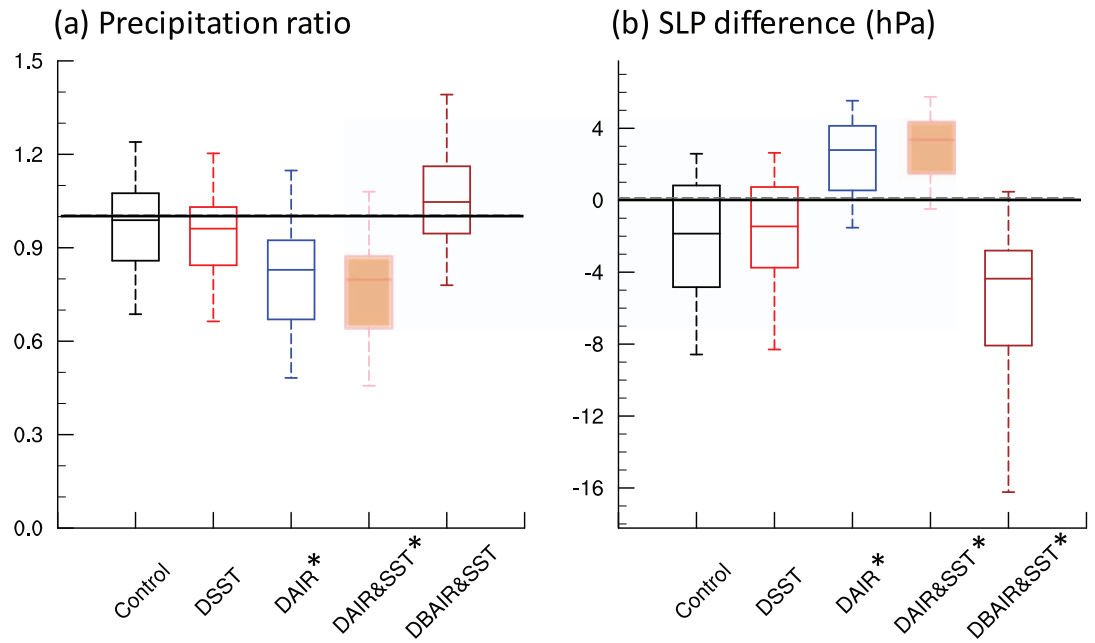

Figure 4. Box and whisker plots of (*a*) the ratio of simulated precipitation and (*b*) minimum sea level pressure relative to the observation with 60 ensemble members each, derived from (left to right) control, DSST, DAIR, DAIR+DSST (color filled), and DB runs. The *x*-axis labels marked with * indicate a significant difference from control runs at 95% confidence interval per *t*-test.

CESM1 LE, after applying the spatial filtering described above to both geopotential height fields. The comparison was made for two domains, a synoptic one for the upper level with low-pass filtering (*ref.* steering conditions and stagnation associated with the low-pressure system in question). It is expected that there would be a range of cases from 'somewhat similar' to 'almost identical' in the historical and simulated data; thus, we designated a range of ρ_P from a low bar of 0.5 (somewhat similar) as the minimal criterion to a high bar of 0.8 (almost identical) with a 0.05 increment for both pressure levels; this led to 49 combinations with seven ρ_P intervals in the upper level pairing to seven ρ_P intervals in the lower level. Furthermore, we applied an intensity criterion using the minimum central value of the 850 h Pa geopotential height. In any 4 day sequence, the daily minimum height within the low-pressure system over southwest Texas (red box in figure 3) had to be at least 0.6 of the value exhibited during 26–29 August 2017. An evaluation made between the reanalysis data and the CESM1 Historical LE yielded a roughly 1:2 ratio of identified cases (not shown). The higher number of cases in CESM1 is expected due to the low-bar criteria that includes extra weaker cases.

The temporal distribution of the identified cases during the 2006–2080 period is presented as a series of box plots in figure 5(*a*) for the number of cases, and in figure 5(*b*) for the four day accumulated precipitation (including all 49 ρ_P combinations per year from each member). A 15 year running mean of their medians is also shown. There is an apparent increase in the number of cases beginning in ~2050, and this is concurrent with event precipitation increases that are projected to continue to ~2070. The Atlantic Ocean has been projected to feature an overall increase in intense tropical cyclone frequency (Jones *et al* 2016), with more category 4–5 storms and fewer weaker storms (Bender *et al* 2010, Knutson *et al* 2010). A warming tropical Atlantic Ocean can induce low-pressure anomalies over the Gulf of Mexico during late summer (Weaver *et al* 2009) and subsequently enhance the conditions for tropical cyclone formation. However, we note that the ability of CESM1 to simulate and project tropical cyclones is unclear, and we do not have a definitive explanation for the subsequent decline after 2070 other than referring it to internal variability. Likewise, the 2050–2070 increase also could be due to internal variability, though the overall uptrends in precipitation and case number from 2020 to 2080 are arguably attributable to climate warming. Here, as was the case in the WRF-ARW simulations, we caution that the projection results in figure 5 may differ by model and by the physics schemes used.

5. Discussion

The reason for the increasing number of low-pressure systems in the Gulf Coast (figure 5(*a*)) is manifold, involving both natural and anthropogenic origins. Some modeling studies project that North Atlantic category 4–5 storms will increase (Bender *et al* 2010, Knutson *et al* 2013) while weaker hurricanes will likely decrease (Jones *et al* 2016). To our knowledge, no studies have focused specifically on future tropical cyclone strength in the Gulf of Mexico, except for a loose comparison made in van der Wiel *et al* (2017). Given

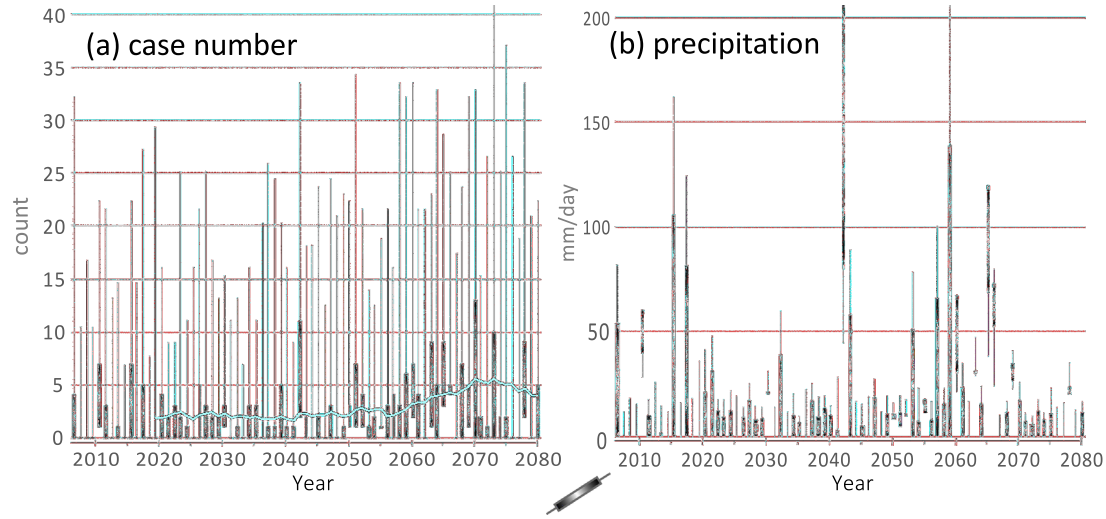

Figure 5. Box and whisker plots of (*a*) the case number accumulated and (*b*) event precipitation averaged over southeast Texas of Harvey-like weather systems depicted from the CESM LE projection data from the ensemble of 40 members for each year. The medians are connected by thick solid line by the backward 15 year moving average.

the widened increase in the number of cases (figure 5(*a*)) between low-bar criteria and high-bar criteria, it is possible that the increase in storm precipitation is mainly driven by weaker tropical cyclones in the Gulf of Mexico.

High moisture content in the atmosphere plays an important role in strong hurricanes like Harvey as well as the storms leading to the 2016 Louisiana flood (Wang *et al* 2016). Precipitable water in the Gulf of Mexico has increased considerably and will only increase in a warming climate; this was both observed and projected by CESM1 as shown in figure 2(*c*). Consequently, the prospect of future tropical cyclones resulting in extreme precipitation is a scenario that the Gulf Coast and coastal metropolitan areas will likely face in the future, and the simulation results of figure 5(*b*) also suggest it. Nonetheless, recent climate projection studies (Gao *et al* 2012, Janssen *et al* 2014, Wuebbles *et al* 2014) did not underscore the Gulf States as a hotspot for a significant increase in summertime extreme precipitation. High-emission climate projections showed only a weak increase in the maximum daily precipitation in Texas and Louisiana, considerably less than the northeast US and Midwest (Wuebbles *et al* 2014); this apparent discrepancy between the two projections requires caution in interpretation.

Conceptually, our approach that constrains the boundary and initial conditions of an atmospheric model used to create a synoptic event is in line with the emerging 'storyline approach' of attribution analysis (Zappa and Shepherd 2017). When it comes to attribution analysis, the mere use of observational data and model free runs is not adequate enough to reach robust conclusions. Global model free runs may approximate a historical hurricane, e.g. as in the Hurricane Sandy attribution (Lackmann 2015), but they do not necessarily replicate the environmental conditions associated with the particular storm. Using the dynamical downscaling approach forced by observed IC and LBC provides the closest possible influences of the true environmental conditions at the time of a mesoscale or weather system of interest. While the simulations suggest that Harvey's precipitation over southeast Texas as well as its intensity could have been enhanced by climate warming trends, we acknowledge that the estimate can change depending on a number of factors, such as different models used and their settings, different IC and LBC sources, and choice of trend periods removed.

6. Conclusion

While the Gulf Coast is no stranger to strong hurricanes, a tropical cyclone that stalls for days over a major metropolitan area and results in excessive rainfall is a recipe for disaster. Quantitative attribution conducted by WRF-ARM downscaling simulations, with the climate trends removed from the IC and LBC, suggest that post-1980 warming in both the ocean and atmosphere likely resulted in a ~20% increase of the accumulated event precipitation with an interquartile range of 13%–37%. Preliminary CESM1 analysis projecting stalled storms over southwest Texas, in conjunction with recent analyses of a similarly stalled storm in Louisiana (van der Wiel *et al* 2017, Wang *et al* 2016), signifies an increasing trend in the number of cases that have similar synoptic patterns and associated stationarity to that of Harvey. Precipitation associated with these stalled storms was also projected to increase, despite CESM1's relatively coarse resolution prevents a more quantitative assessment.

The method demonstrated here echoes one of the alternative ways outlined in Trenberth *et al* (2015) to resolve the challenge facing attribution analysis from a physical standpoint, that is, questioning whether observed changes in the thermodynamic state affected the impact of a particular event. We note that the post-1980 warming is not simply due to anthropogenic causes but also likely involves natural climate variability and random weather systems. Risser and Wehner (2017) conducted extreme value analysis using CO_2 concentration and annually-averaged El Niño–Southern Oscillation (ENSO) as covariates and found that human-induced climate change likely increased Harvey's precipitation in the Houston metropolitan area by 40% with a lower bound estimate of 18%. We note, however, similarly to what they acknowledged in their paper, that other natural modes of variability such as the AMO may be responsible for some of the increase in SST in the Gulf of Mexico. In the context of event attribution, our regional downscaling attribution approach went one step further in conducting a more direct, 'apples-to-apples' comparison of Harvey's extreme precipitation when compared to the value-based (not event-specific) statistical analysis or return period analysis that relies on capturing similar 'Harvey-like' events, without dealing with the environment factors and synoptic settings accompanying the particular event of interest. In general, our result is in agreement with that of van Oldenborgh *et al* (2017) and Emanuel (2017) in that anthropogenic warming in the atmosphere contributed to the rainfall intensity of Harvey and may lead to more frequent similar storms in the future.

The estimate from the present downscaling attribution is by no means absolute and attributing convectively-driven extreme precipitation events is challenging. Our purpose here is not necessarily to provide a definitive number but rather to propose a way to provide a more direct, quantitative measure for conducting extreme precipitation event attribution. For a better representation of storm-scale structures in organized convective systems, the US Climate Variability and Predictability Program (CLIVAR) suggest future research to consider utilizing convective permitting modeling that shows superior performance in warm-season convection (US_CLIVAR 2017). We thus call for a careful reevaluation of the projection of both tropical cyclones and other convective systems that may become more stalled in the future and produce more rainfall.

Acknowledgments

S W was supported by the SERDP grant RC-2709. J Y was supported by the GIST Research Institute (GRI) Grant funded by the GIST in 2018. P K would like to acknowledge funding from the G Unger Vetlesen Foundation.

ORCID iDs

Jin-Ho Yoon https://orcid.org/0000-0002-4939-8078

References

Bender M A, Knutson T R, Tuleya R E, Sirutis J J, Vecchi G A, Garner S T and Held I M 2010 Modeled impact of anthropogenic warming on the frequency of intense Atlantic hurricanes *Science* **327** 454–8

Blake E S and Zelinsky D A 2018 *National Hurricane Center Tropical Cyclone Report: Hurricane Harvey* (Miami, FL: N H Center) p 76

Cho C, Li R, Wang S-Y, Yoon J-H and Gillies R R 2016 Anthropogenic footprint of climate change in the June 2013 northern India flood *Clim. Dyn.* **46** 797–805

Emanuel K 2017 Assessing the present and future probability of Hurricane Harvey's rainfall *Proc. Natl Acad. Sci.* **114** 12681–4

Enfield D B, Mestas-Nuñez A M and Trimble P J 2001 The Atlantic Multidecadal Oscillation and its relation to rainfall and river flows in the continental US *Geophys. Res. Lett.* **28** 2077–80

Gao Y, Fu J, Drake J, Liu Y and Lamarque J 2012 Projected changes of extreme weather events in the eastern United States based on a high resolution climate modeling system *Environ. Res. Lett.* **7** 044025

Hart R E, Chavas D R and Guishard M P 2016 The arbitrary definition of the current Atlantic major hurricane landfall drought *Bull. Am. Meteorol. Soc.* **97** 713–22

Janssen E, Wuebbles D J, Kunkel K E, Olsen S C and Goodman A 2014 Observational-and model-based trends and projections of extreme precipitation over the contiguous United States *Earth's Future* **2** 99–113

Jones J J, Stephenson T S, Taylor M A and Campbell J D 2016 Statistical downscaling of North Atlantic tropical cyclone frequency and the amplified role of the Caribbean low-level jet in a warmer climate *J. Geophys. Res.: Atmos.* **121** 3741–58

Kanamitsu M, Ebisuzaki W, Woollen J, Yang S-K, Hnilo J J, Fiorino M and Potter G L 2002 NCEP–DOE AMIP-II Reanalysis (R-2) *Bull. Am. Meteorol. Soc.* **83** 1631–43

Kay J *et al* 2015 The community earth system model (CESM) large ensemble project: a community resource for studying climate change in the presence of internal climate variability *Bull. Am. Meteorol. Soc.* **96** 1333–49

Knutson T R *et al* 2010 Tropical cyclones and climate change *Nat. Geosci.* **3** 157–63

Knutson T R *et al* 2013 Dynamical downscaling projections of twenty-first-century Atlantic Hurricane activity: CMIP3 and CMIP5 model-based scenarios *J. Clim.* **26** 6591–617

Lackmann G M 2015 Hurricane Sandy before 1900 and after 2100 *Bull. Am. Meteorol. Soc.* **96** 547–60

Lin Y and Mitchell K E 2005 The NCEP Stage II/IV hourly precipitation analyses: development and applications *19th Conf. on Hydrology, American Meteorological Society* paper 1.2

Risser M D and Wehner M F 2017 Attributable human-induced changes in the likelihood and magnitude of the observed extreme precipitation during Hurricane Harvey *Geophys. Res. Lett.* **44** 12,457–64

Skamarock W C and Klemp J B 2008 A time-split nonhydrostatic atmospheric model for weather research and forecasting applications *J. Comput. Phys.* **227** 3465–85

Trenberth K E, Fasullo J T and Shepherd T G 2015 Attribution of climate extreme events *Nat. Clim. Change* **5** 725

US_CLIVAR 2017 US CLIVAR Summit Report 38 (https://doi.org/10.5065/D5066CJ5068C5064)

van der Wiel K *et al* 2017 Rapid attribution of the August 2016 flood-inducing extreme precipitation in south Louisiana to climate change *Hydrol. Earth Syst. Sci.* **21** 897–921

van Oldenborgh G J *et al* 2017 Attribution of extreme rainfall from Hurricane Harvey, August 2017 *Environ. Res. Lett.* **12** 124009
Wang S-Y, Zhao L and Gillies R R 2016 Synoptic and quantitative attributions of the extreme precipitation leading to the August 2016 Louisiana flood *Geophys. Res. Lett.* **43** 11,805–814
Weaver S J, Schubert S and Wang H 2009 Warm season variations in the low-level circulation and precipitation over the Central United States in observations, AMIP simulations, and idealized SST experiments *J. Clim.* **22** 5401–20
Weaver S J, Kumar A and Chen M 2017 Recent increases in extreme temperature occurrence over land *Climate Extremes* (New York: Wiley) pp 105–14
Wuebbles D J *et al* 2014 CMIP5 climate model analyses: climate extremes in the United States *Bull. Am. Meteorol. Soc.* **95** 571–83
Zappa G and Shepherd T G 2017 Storylines of atmospheric circulation change for european regional climate impact assessment *J. Clim.* **30** 6561–77